Bioorganic & Medicinal Chemistry 20 (2012) 2796–2802

Contents lists available at SciVerse ScienceDirect

Bioorganic & Medicinal Chemistry

journal homepage: www.elsevier.com/locate/bmc

Solution NMR analysis of the binding mechanism of DIVS6 model peptides of voltage-gated sodium channels and the lipid soluble alkaloid veratridine

Ai Yoshinaka-Niitsu [a], Tohru Yamagaki [a,b,*], Masanori Harada [a], Kazuo Tachibana [a]

[a] Department of Chemistry, School of Science, The University of Tokyo, 7-3-1 Hongo, Bunkyo, Tokyo 113-0033, Japan
[b] Suntory Institute for Bioorganic Research, 1-1-1 Wakayamadai, Shimamoto, Mishima, Osaka 618-8503, Japan

ARTICLE INFO

Article history:
Received 2 February 2012
Revised 14 March 2012
Accepted 15 March 2012
Available online 23 March 2012

Keywords:
Neurotoxic alkaloid
Sodium channel
Interaction mechanism
NMR
Model peptides

ABSTRACT

Voltage-gated sodium channels (VGSCs) are responsible for generating action potentials in nervous systems. Veratridine (VTD), a lipid soluble alkaloid isolated from sabadilla lily seed, is believed to bind to segment 6 of VGSCs and act as a partial agonist. However, high resolution structural interaction mechanism between VGSCs and VTD is difficult to elucidate because of the large size and membrane localization of VGSCs. Here, the authors designed model peptides corresponding to domain IV segment 6 (DIVS6) of rat skeletal muscle $Na_v1.4$ and analyzed the complex of the model peptides and VTD by solution NMR analysis to obtain structural information of the interaction. The model peptides successfully formed an α-helices, which is the suspected native conformation of DIVS6, in aqueous 2,2,2-trifluoroethanol, a membrane-mimicking solvent. The VTD binding residues of the model peptide were identified using the NMR titration experiments with VTD, including a newly discovered VTD binding residue Leu14 (μ1-L1580 in $Na_v1.4$), which has not been reported by point mutation studies. Mapping of VTD binding residues on the model peptide revealed the hydrophobic interaction surface. NMR titration experiments with a non-toxic analog of VTD, veracevine, also indicated that the steroidal backbone of VTD interacts with the hydrophobic interaction surface of DIVS6 and that the 3-acyl group of VTD possibly causes neurotoxicity by interacting with domain I segment 6 and/or domain IV segment 4.

1. Introduction

Voltage-gated sodium channels (VGSCs) are transmembrane proteins responsible for generating action potentials in nervous systems.[1–4] From gene organization to biophysical properties, there are large similarities between vertebrate and invertebrate VGSCs.[5] Human and rat VGSCs have been most extensively studied, and it is known that mutations in human VGSCs cause channel diseases (channelopathies) such as epilepsy, paramyotonia, and cardiac arrhythmia.[6,7] VGSCs consist of α (260 kDa), β1 (36 kDa), and β2 (33 kDa) subunits, where α subunits are functionally classified in nine groups ($Na_v1.1$–1.9). The primary structure of α subunits consists of four homologous domains, each containing six α-helical segments.[1,4,8] Segment 6 of each domain, which is a transmembrane pore-forming region, is considered to be targeted by neurotoxins and local anesthetics.[4,9]

Segment 6 targeting neurotoxins, veratridine (VTD) **1** and its analog veracevine (VC) **2**, are lipid soluble alkaloids isolated from sabadilla lily seed known collectively as veratrum alkaloids.[10,11] VTD, which is composed of a steroidal backbone and the 3-acyl group, activates VGSCs as a partial agonist and is neurotoxic. In contrast, VC, which is composed of the steroidal backbone and the 3-hydroxyl group, is non-toxic. Previous research has shown that the 3-acyl group is essential for VTD neurotoxicity,[12] and we have previously suggested that the steric conformation of the 3-acyl group is an important factor in neurotoxicity.[13] A competitive binding study of VTD and radiolabeled batrachotoxin **3** (BTX, Fig. 1), a full agonist of VGSCs, and point mutation studies led to the conclusion that VTD and BTX share a common binding site on segment 6 categorized as "site-2".[9,14–16] Domain IV segment 6 (DIVS6) has the largest number of interactive residues among the four segment 6s, which was suggested by point mutation experiments using the rat skeletal muscle $Na_v1.4$.

It has been suggested that structural information for the interaction mechanisms between VTD and VGSCs can help clarify functions and structural features of VGSCs, and aid the search for new therapies for neuronal diseases.[16–18] Recently, the crystal structure of a bacterial homotetramer VGSC from *Arcobacter butzleri* has been reported.[19] However, the high resolution structure of VGSCs with four linked domains has not been clarified because of their

Abbreviations: CD, circular dichroism; DQF-COSY, double-quantum filtered-correlation spectroscopy; MALDI-TOF MS, matrix-assisted laser desorption/ionization time-of-flight mass spectrometry; NOESY, nuclear overhauser enhancement and exchange spectroscopy; TFE, trifluoroethanol; TOCSY, total correlation spectroscopy.

* Corresponding author. Tel.: +81 75 962 7094; fax: +81 75 962 2115.
E-mail address: yamagaki@sunbor.or.jp (T. Yamagaki).

0968-0896/$ - see front matter © 2012 Elsevier Ltd. All rights reserved.
http://dx.doi.org/10.1016/j.bmc.2012.03.034

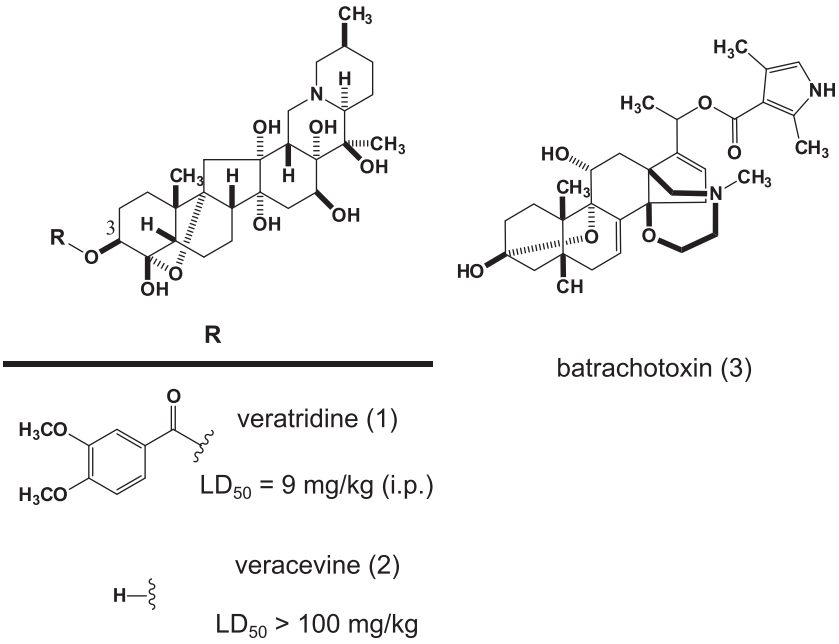

Figure 1. Chemical structures of veratridine (**1**), veracevine (**2**), and batrachotoxin (**3**). LD_{50} of veratridine and veracevine were estimated by mouse lethality with intraperitoneal injection (ip).

large size and membrane localization. To characterize interaction mechanisms of neurotoxins and VGSCs while avoiding these problems, the approach of the interaction analysis by solution NMR using the complex of an isolated segment of VGSCs, the DIV/S3-S4 loop, with its ligands has been successfully demonstrated.[20] In the report, isolation of the VGSC segment, which means downsizing of the target, enabled structural analysis of the interaction by NMR analysis.

In this study, to perform direct structural analysis of the interaction between a neurotoxin and a transmembrane segment of VGSCs by solution NMR analysis, we applied the above-mentioned approach to the complex of VTD and transmembrane model peptides (TMPs) corresponding in amino acid sequence to DIVS6 in aqueous 2,2,2-trifluoroethanol (TFE). The aqueous TFE, which has been used recently as a membrane-mimicking condition,[21–23] was selected to enable solution NMR analysis of the transmembrane segment. NMR structures of synthesized TMPs were investigated by solution NMR data and structure calculations, and the interaction between VTD and TMPs was analyzed by NMR titration experiments.

2. Materials and methods

2.1. Peptide synthesis

Native sequence of DIVS6 of $Na_v1.4$ is ^{1567}GICFFCSYIIISFLIVVNM YIAIILENF^{1594}. In the present study, amino acid residues of DIVS6 were numbered as G_1–F_{28} and those of model peptides were numbered to follow the corresponding positions to DIVS6 as TMP1 (^{7}SKIIKSFLKVVNKYIAIILE^{26}-NH_2) and TMP2 (^{3}KKKSYIIISFLIVV NMYIAIILEKKK^{29}-NH_2). TMP1 and TMP2 were synthesized on a solid-phase peptide synthesizer (PIONEER™ Peptide Synthesis System, Applied Biosystems, CA, USA) at a 0.1 mmol scale. Deprotection and cleavage from resin were performed using a trifluoroacetic acid/water (9.5/0.5, v/v).

TMPs were purified by reversed-phase HPLC (JASCO HPLC System; Jasco Corp., Hachioji, Japan) on a $5C_4$-AR300 column (20φ × 250 mm; Nacalai Tesque, Kyoto, Japan) for TMP1 and on a YMC-Pack C4-AP-823 300A column (10φ × 250 mm; YMC Co., Ltd, Kyoto, Japan) for TMP2. A water/acetonitrile linear gradient with 0.1% trifluoroacetic acid was used for purification. The purity of each peptide was determined using MALDI-TOF MS (AXIMA-CFRs; Shimadzu, Co., Kyoto, Japan) (Supplementary Figs. 1 and 2).

2.2. Preparation of veratridine and veracevine

Veratridine was purchased from Sigma–Aldrich, Japan and used without further purification. Veracevine was prepared from veratridine by alkaline hydrolysis as previously described.[13]

2.3. CD measurements

CD measurement was performed using a JASCO J-725 spectrometer (Jasco Corp.) with a cuvette of 1 mm path length. TMP1 and TMP2 were dissolved in a TFE/H_2O mixture (1/1, v/v) at 0.288 mM and 0.162 mM, respectively. Each spectrum was recorded with 10 scans.

2.4. NMR sample preparation

All NMR samples were dissolved in 200 μL of TFE-d_2/H_2O mixture (1/1, v/v). For titration experiments, 18.6 mM solutions each of veratridine and veracevine were prepared. For the titration of TMP1 with VTD or VC, VTD/VC solution was added to 2.2 mM TMP1 solution up to 0.75 equiv to TMP1. For titration of TMP2 with VTD, VTD solution was added to 0.75 mM TMP2 solution up to 1 equiv to TMP2.tp

2.5. NMR measurement

^{1}H, TOCSY, NOESY, and DQF-COSY spectra were measured on a JEOL ECA 500 MHz spectrometer with nanolac probes (^{1}H, 500 M Hz; JEOL Ltd, Tokyo, Japan). All NMR spectra were obtained at 25 °C. Mixing time was 120 ms for TOCSY and 400 ms for NOESY. NMR data were processed and analyzed using Delta (version 4.3.6; JEOL Ltd)

2.6. Structure calculation

The simulated annealing software package XPLOR-NIH (version 2.21) was used for structure calculation.[24,25] Distance restraints derived from NOE peak intensities in NOESY spectra and dihedral angle restraints derived from coupling constants in DQF-COSY spectra were used to refine the structure. The structures were obtained from simulated annealing (20 times) with subsequent refinement and acceptance steps. Calculated structures were viewed on VMD with LINUX (version 1.8.5).[26]

2.7. Dissociation constant calculation

Dissociation constants of TMPs and veratrum alkaloids were estimated by least-square curve fitting by using the Marquardt & Levenberg algorithm on Graph Pad Prism (version 3.02; GraphPad Software, Inc., CA). The constants for TMP1 and TMP2 were calculated from plotting chemical shift change of the amide protons of Val17 and Lys5 as functions of VTD or VC concentrations, respectively.

3. Results and discussion

3.1. Design and preparation of TMPs

Because the transmembrane segment, DIVS6, of the whole channel protein is expected to form an α-helix in the biomembrane system,[1,4,8] TMPs should be designed to form an α-helix in 50% aqueous TFE as a membrane-mimicking condition.[21–23] The designed TMPs had lysine residues to increase their solubility and were synthesized chemically on solid phase. Their α-helix formation was evaluated using CD spectroscopy in 50% aqueous TFE.

First, the TMP with the native DIVS6 sequence (Fig. 2) was synthesized and the target peptide was detected by MALDI-TOF MS (Supplementary Fig. 3); however, the solubility was too low to allow purification by HPLC. Next, a model peptide in which two lysine residues were added to each terminus of the DIVS6 sequence Ser7-Glu26 was synthesized (Supplementary Fig. 4), but the TMP solubility was as poor as that of the native DIVS6 sequence. Finally, two TMPs with adequate solubility were designed (Fig. 2). The four amino acid residues of DIVS6—Tyr8, Ile11, Ile15, and Met19—were replaced with lysines as shown for TMP1. The replaced four Lys residues were expected to align on the same surface when TMP1 formed the α-helix. This is an important concept, that the hydrophilic Lys surface is located on the opposite side of the amino acid residues essential for the interaction of DIVS6 and VTD in the α-helix formation (Fig. 2b). Similar to TMP1, TMP2 was designed by adding three lysines to each terminus of Ser7-Glu26 (Fig. 2c). TMP1 and TMP2 were synthesized and purified with satisfactory yields.

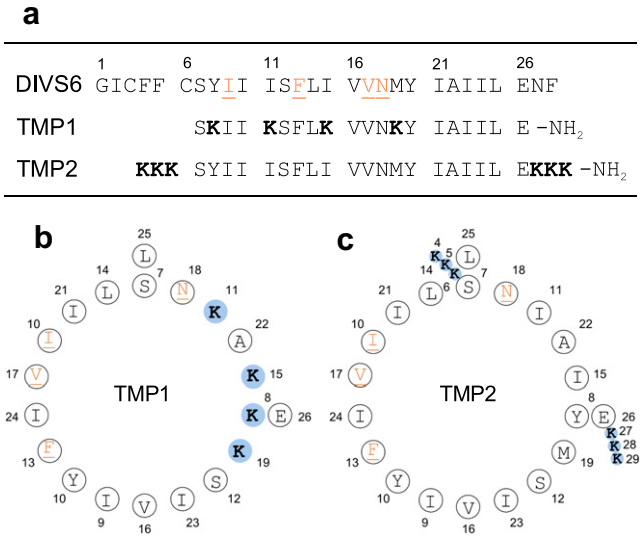

Figure 2. (a) Amino acid sequences of DIVS6 and TMPs. (b)and(c) Helical wheels of TMP1 and TMP2. Suggested VTD binding residues from point mutation experiments are underlined. Added lysines are in bold.

To evaluate secondary structures of TMPs in 50% aqueous TFE, the purified TMPs were subjected to CD measurement. Formation of α-helix was characterized with local minimums at 208 nm and 222 nm in CD spectra.[27] Because both TMP1 and TMP2 in 50% TFE showed the characteristic α-helical pattern in the CD spectra (Supplementary Fig. 5), TMP1 and TMP2 were confirmed to form α-helices in most regions. Consequently, subsequent NMR measurements were performed in a 50% TFE solvent system to determine conformations of each residue.

3.2. Spectral assignment and structure determination of TMPs

Figure 3 shows the TOCSY spectra of TMPs in TFE-d_2/H_2O mixture (1/1, v/v). The signals of the amide protons and the alpha protons were assigned by sequence specific assignment using TOCSY and NOESY spectra[28] (Fig. 3a,b), and subsequently the signals of the side chains were also assigned on TOCSY spectra. The NOE correlations among $d_{\alpha N}(i, i+3)$, $d_{\alpha N}(i, i+4)$, and $d_{\alpha\beta}(i, i+3)$ were observed (Fig. 3c,d), and they indicated α-helix formation of TMPs.[29] The NOE connectivity patterns in Figure 3 indicated that TMPs formed α-helices in almost all regions.

Simulated annealing calculations were performed for structure determination of TMPs using software package XPLOR-NIH with constraints from NMR data.[24,25] Distance restraints derived from NOE peak intensities and dihedral angle restraints derived from coupling constants were used to refine the structure. Refined and accepted structures of TMP1 and TMP2 were determined by repeated calculations (20 times).

Superimposed structures of TMP1 (Fig. 4a) indicated that the center part of the peptide forms an α-helix and the N-terminus does not converge to a single conformation. The structures of TMP2 (Fig. 4b) indicated that the three N-terminal lysine residues do not form an α-helix and are slightly fluctuating. In both TMP1 and TMP2, the obtained structures indicated that most regions with native amino acid sequences form α-helices as the expected native conformation. Therefore, we confirmed that TMP1 and TMP2 had reasonable and ideal properties as model peptides for analysis of the interaction mechanism between VTD and DIVS6 by solution NMR analysis.

3.3. VTD binding site mapping by titration experiments

The VTD binding sites of TMPs were analyzed by comparing TOCSY spectra of TMPs with or without VTD. In the titration experiment of TMP1 with VTD, chemical shift perturbations were observed in the NH-αH region and in the side chain region, and the amide proton signal of Lys8 disappeared (Fig. 5a,b). The disappearance of the Lys8 signal suggested that the structure of the N-terminus part of TMP1 was indirectly changed by VTD binding. Because the signal changes of Lys8 and the surrounding residues Lys11 and Ser12 were considered to be induced by the structural changes of TMP1 rather than VTD binding, these residues were removed from candidate VTD binding sites. Amide protons of Ile9, Ile10, and Leu14 exhibited large (>0.03 ppm) chemical shift changes (Fig. 6a), and the TOCSY cross peaks of Ile10, Val16, and Asn18 were perturbed both in the amide proton and side chain regions (Figs. 5and6a). Consequently, Ile9, Ile10, Leu14, Val16, and Asn18 were identified as the residues likely responsible for VTD binding.

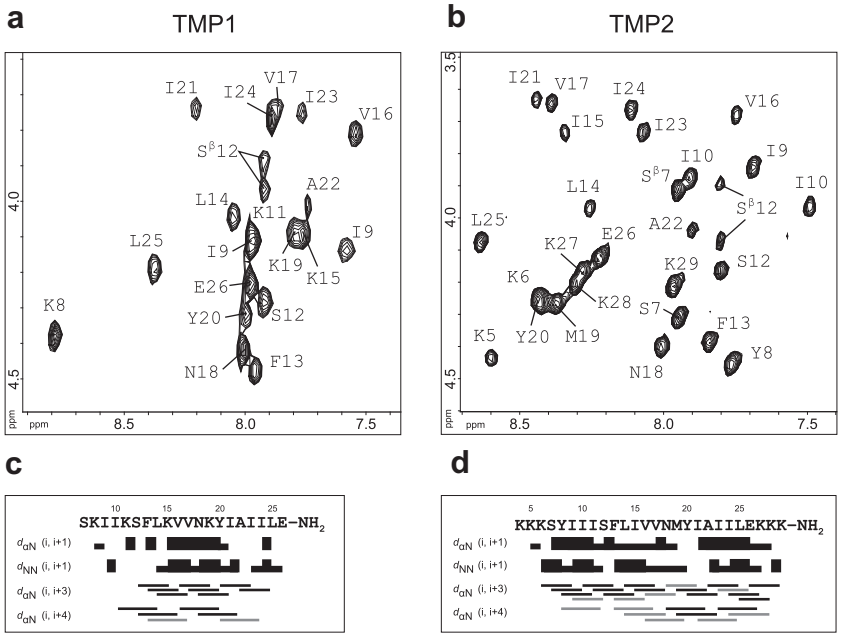

Figure 3. Signal assignments in the NH-αH region of TOCSY spectra of (a) TMP1 and (b) TMP2, and NOE connectivity tables of (c) TMP1 and (d) TMP2. In NOE connectivity tables, bar height depicts the intensity of correlation peaks in rows of $d_{\alpha N}(i, i+1)$ and $d_{NN}(i, i+1)$. Black bars indicate clear NOEs, and gray bars represent ambiguous NOEs in rows of $d_{\alpha N}(i, i+3)$ and $d_{\alpha N}(i, i+4)$.

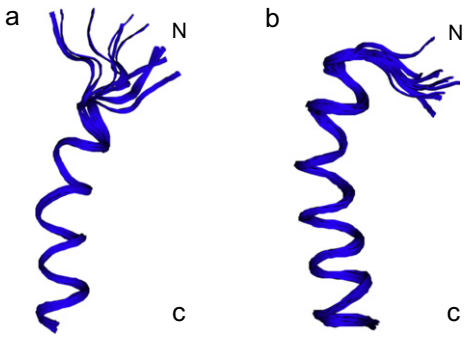

Figure 4. Ten superimposed structures of refined (a) TMP1 and (b) TMP2 obtained by repeated calculations (20 times).

These residues were mapped on the calculated structure of TMP1 as shown in Figure 7a. Because the mapped residues are located on the hydrophobic surface of TMP1, the surface could be involved in the interaction with VTD. Furthermore, the amino acid residues Ile9, Phe13, Val17, and Asn18, which were identified as essential for VTD binding to DIVS6 by previous point mutation experiments, were mapped on TMP1 (Fig. 7b). Chemical shift perturbation was observed at all four residues in the titration experiments. This agreement suggested that TMP1 can interact with VTD in a manner similar to that for DIVS6 and VTD. Thus, the expected VTD binding site on TMP1 was located by mapping the residues that significantly changed in chemical shift and that agreed with point mutation experiments (Fig. 7c). The result of mapping strongly indicated that the hydrophobic surface that the mapped residues form on TMP1 is essential for VTD binding in VGSCs.

In the titration experiment of TMP2 with VTD (Fig. 5c), the chemical shift perturbation of TMP2 in the NH-αH region was much smaller than that of TMP1 (Fig. 6b). Because the N-terminus of TMP2 does not form α-helical conformation, as shown in the calculated structure, amino acid residues around the N-terminus are not included in the discussion of the VTD binding site. Apart from the N-terminus, chemical shift perturbation at Leu14 and Ile15 were expected to be caused by direct VTD interaction (Fig. 6b). Of note, chemical shift perturbation at the amide proton of Leu14 was observed in both TMP1 and TMP2. Leu14 was located in the VTD binding surface of TMP1, suggesting that it is a key residue for binding between VTD and TMPs. Leu14 of TMPs is L1580 in the sequence of the rat skeletal muscle VGSC, $Na_v1.4$ (μ1). In point mutation experiments, μ1-L1580 has not been included among the residues required for binding (Fig. 2). However, our NMR experiments suggest that μ1-L1580 is indeed a part of the VTD binding site.

3.4. Interaction mechanism between VTD and DIVS6

To determine the manner of VTD binding, the dissociation constants of the TMP–VTD/VC complexes were determined by least-squares curve fitting to the changes of chemical shift as a function of ligand concentration by using the Marquardt & Levenberg algorithm (Fig. 8). The chemical shift changes fit well to the one-site binding curve, which indicates one-site binding of TMPs and veratrum alkaloids.

Titration experiments of TMP1 with VC, which is a non-toxic analog of VTD, showed a similar chemical shift perturbation pattern as that of the TMP1/VTD experiments at the NH-αH region of the TOCSY spectra (Fig. 5c). Dissociation constants of VTD and VC from TMP1 were in the same order, 1 mM (Fig. 8a). These consistencies suggest that VTD and VC interact with TMP1 in the same manner. VTD and VC share the common steroidal backbone, and VTD has the 3-acyl group that plays an important role in the neurotoxicity of veratrum alkaloids.[12] These structural features and titration experiments using VTD and VC suggested that the steroidal backbone of VTD is important for the interaction with DIVS6 and that channel activation can be induced by binding of the 3-acyl group to other segments. The steroidal backbone of veratrum alkaloids is highly hydrophobic, and the mapped VTD binding site of TMP1 formed a hydrophobic surface (Fig. 7c). The sizes of these

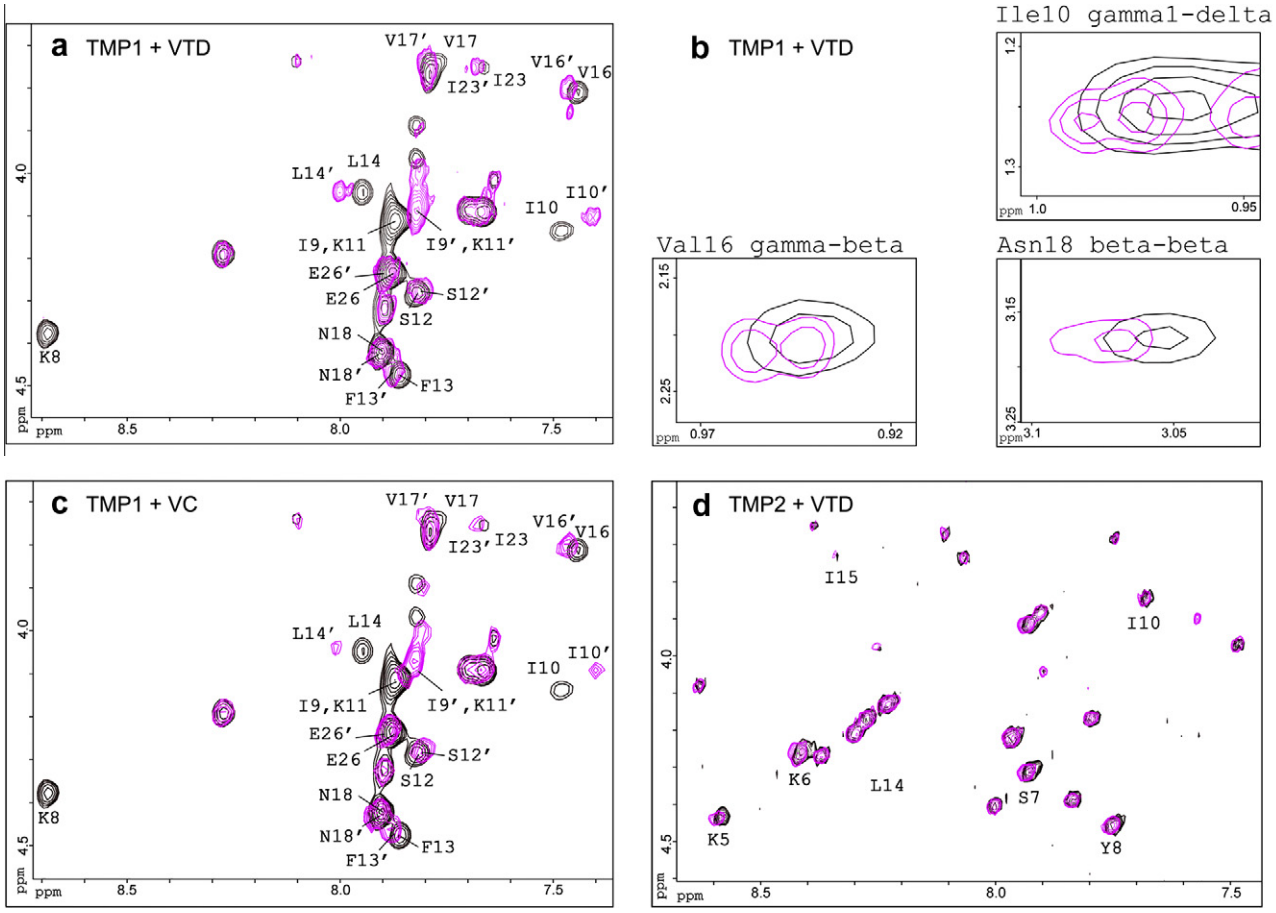

Figure 5. Superimposed TOCSY spectra of titration experiments at 25 °C, 500 MHz. Spectra of the peptide alone are represented by black lines and that of the peptide with VTD or VC are represented by magenta lines. (a) NH-αH region, TMP1 and TMP1 with 0.62 equiv of VTD. (b) Side chain signals, TMP1 and TMP1 with 0.62 equiv of VTD. (c) NH-αH region, TMP1 and TMP1 with 0.62 equiv of VC. (d) NH-aH region, TMP2 and TMP2 with 1.0 equiv of VTD.

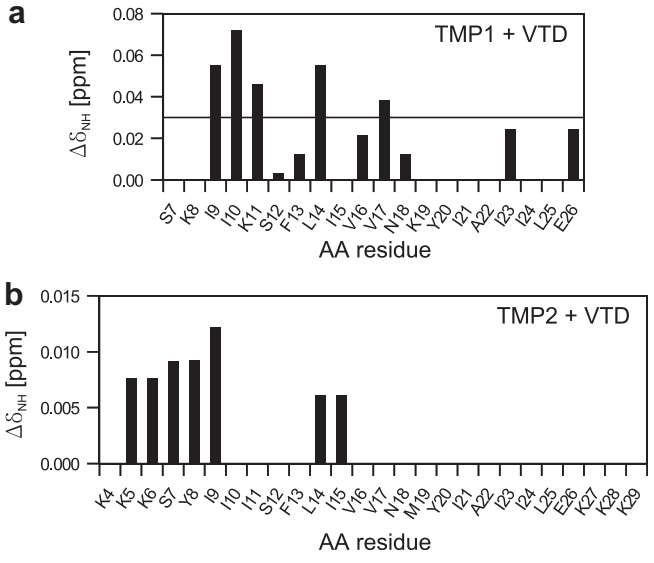

Figure 6. Chemical shift changes of amide protons of (a) TMP1 and (b) TMP2.

surfaces, approximately 11 Å, confirm the hydrophobic interaction between the steroidal backbone and DIVS6.

The interaction mechanism of VTD suggested by this research is consistent with the expected interaction mechanism from competitive binding studies with BTX and point mutation studies. Regarding the BTX interaction mechanism, photo-active derivatives of BTX containing ^{3}H and an azide group at the aromatic acyl group exhibited covalent labeling to DIS6.[14] Point mutations at DIVS6 reduced the binding affinity of BTX to VGSCs.[30,31] These reports proposed a domain–interface model of BTX binding to the interface between domain I segment 6 (DIS6) and DIVS6.[4] VTD is expected to share a common binding site with BTX and thereby interact with VGSCs in a similar domain–interface mechanism.[9,14–16] DIS6 is a candidate binding target of the 3-acyl group. On the other hand, BTX and VTD are also expected to induce persistent activation at resting membrane potential via an allosteric mechanism that leads to the blockage of sodium channel inactivation.[30] BTX and VTD binding to DIVS6 may change the voltage-dependent movements of the adjacent DIVS4, which is a voltage-sensor segment and affects both activation and coupling of activation to inactivation.[4,30] Therefore, DIVS4 can also be an important factor of the interaction mechanism. BTX and VTD structures have similarities; however, aromatic esters of the two compounds are located on opposite sides when rigid oxygen triangles of their structures are superimposed,[32] which suggests that the 3-acyl group of VTD may interact not only with DIS6 but also with DIVS4. Our results provide evidence for the domain–interface interaction mechanism of VTD, suggesting that VTD binds to DIVS6 with the steroidal backbone and to other segments, such as DIS6 or DIVS4, with the 3-acyl group (Fig. 9). Moreover, the binding affinity between the identified interaction surface of DIVS6 and steroidal backbones can be a new guide for designing channel pore-targeting drugs.

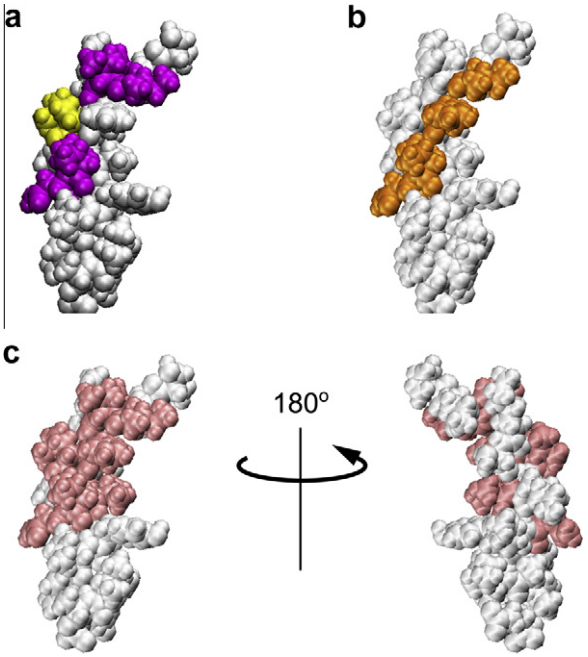

Figure 7. VTD interaction site mapping on the structure of TMP1. (a) Amino acid residues where chemical shift perturbation was observed at both amide proton and side chain regions of TOCSY spectra or with >0.03 ppm change are represented in magenta. Leu14, which exhibited chemical shift perturbation in both TMP1 and TMP2, is represented in yellow. (b) Four amino acid residues—Ile9, Phe13, Val17, and Asn18—which are suggested as VTD binding sites by point mutation studies, are represented in orange. (c) VTD interaction residues suggested by the present study are represented in light pink.

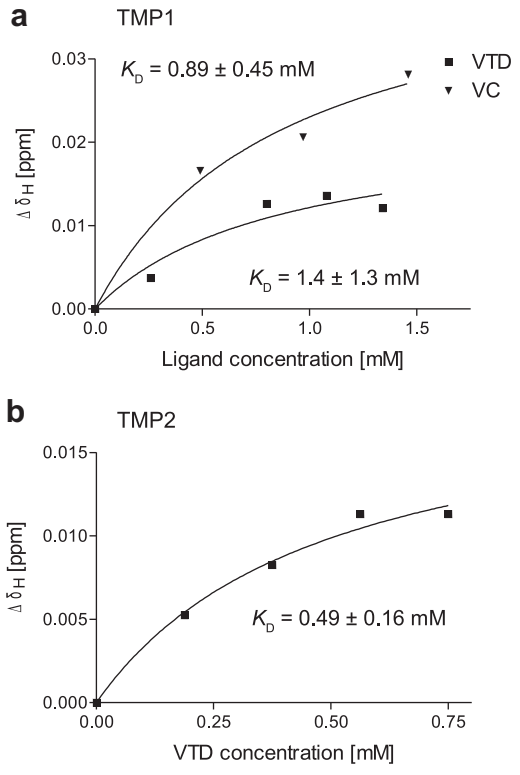

Figure 8. Chemical shift changes of TMPs as a function of increased VTD (■) or VC (▼) concentrations. Dissociation constants were estimated by least-square curve fitting with the Marquardt & Levenberg algorithm on Graph Pad Prism (version 3.02). (a) Chemical shift changes of Val17 amide proton of TMP1. (b) Chemical shift changes of Lys5 amide proton of TMP2.

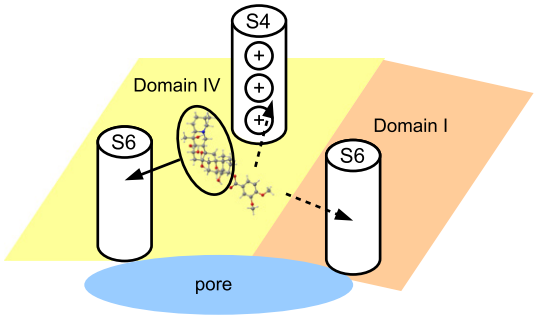

Figure 9. A suggested interaction model of VTD and transmembrane segments. The steroidal backbone of VTD can interact with DIVS6 and the 3-acyl group may interact with DIVS4 or DIS6.

4. Conclusions

We investigated the interaction model of TMPs, which correspond to DIVS6 of the VGSC $Na_v1.4$, and VTD in a membrane-mimicking solvent by NMR titration experiments. Mapping the results of titration experiments on the calculated structure identified the hydrophobic VTD binding surface, which included VTD binding residues suggested by previous point mutation experiments of $Na_v1.4$, and a newly suggested binding site, Leu14 (μ1-L1580 in $Na_v1.4$). The consistency of the chemical shift perturbation pattern caused by VTD and VC on TMP1 indicated that the steroidal backbone of VTD can interact with DIVS6, and channel activation can be induced by interaction of the 3-acyl group to other segments located near DIVS6, such as DIVS4 or DIS6. The suggested domain–interface interaction was consistent with the interaction mechanism predicted by previous biochemical experiments. Therefore, our model complexes of TMPs and veratrum alkaloids appear to reflect the native interaction manner and provide structural information of the interaction between DIVS6 and VTD. Further investigation of VTD binding to segments surrounding DIVS6 will be able to identify the topology and facing direction of each segment.

Acknowledgments

We thank Dr. Takuhiro Ito (The University of Tokyo) and Dr. Naohiro Kobayashi (Institute for Protein Research, Osaka University) for their advice with structure calculations. We are also very grateful to our laboratory colleague Dr. Takahisa Genji for helpful discussions. This research was financially supported by a Grant-in-Aid for the Japan Society for the Promotion of Science (JSPS) Research Fellows, SUNBOR Grant of Suntory Foundation for Life Sciences, and the Global COE program, Chemistry Innovation, The University of Tokyo.

Supplementary data

Supplementary data associated with this article can be found, in the online version, at http://dx.doi.org/10.1016/j.bmc.2012.03.034.

References and notes

1. Catterall, W. A. *Neuron* **2000**, *26*, 13.
2. Yu, F. H.; Catterall, W. A. *Genome Biol.* **2003**, *4*, 207.
3. Wada, A. J. *Pharmacol. Sci.* **2006**, *102*, 253.
4. Yarov-Yarovoy, V.; Catterall, W. A.; Ceste, S.; Yu, F. H.; Konoki, K.; Scheuer, T. *Toxicon* **2007**, *49*, 124.
5. Plummer, N. W.; Meisler, M. H. *Genomics* **1999**, *57*, 323.
6. Hubner, C. A.; Jentsch, T. J. *Hum. Mol. Genet.* **2002**, *11*, 2435.
7. Catterall, W. A.; Dib-Hajj, S.; Meisler, M. H.; Pietrobon, D. *J. Neurol.Sci.* **2008**, *28*, 11768.
8. Guy, H. R.; Seetharamulu, P. *Proc. Natl. Acad. Sci. U.S.A.* **1986**, *83*, 508.

9. Wang, S. Y.; Wang, G. K. *Proc. Natl. Acad. Sci. U.S.A.* **1998**, *95*, 2653.
10. Pelletier, S.; Jacobs, W. A. *J. Am. Chem. Soc.* **1953**, *75*, 3248.
11. Zang, X.; Fukuda, E. K.; Rosen, J. D. *J. Agric. Food Chem.* **1997**, *45*, 1758.
12. Ujvary, I.; Eya, B. K.; Grendell, R. L.; Toia, R. F.; Casida, J. E. *J. Agric. Food Chem.* **1875**, *1991*, 39.
13. Niitsu, A.; Harada, M.; Yamagaki, T.; Tachibana, K. *Bioorg. Med. Chem.* **2008**, *16*, 3025.
14. Trainer, V. L.; Brown, G. B.; Catterall, W. A. *J. Biol. Chem.* **1996**, *271*, 11261.
15. Wang, G. K.; Quan, C.; Seaver, M.; Wang, S. Y. *Pflugers Arch.* **2000**, *439*, 705.
[16]. Wang, S.; Wang, G. K. *Cell. Signal.* **2003**, *15*, 151.
17. Anger, T.; Madge, D. J.; Mulla, M.; Riddall, D. *J. Med. Chem.* **2001**, *44*, 115.
18. Arias, H. R. *Mar. Drugs* **2006**, *4*, 37.
19. Payandeh, J.; Scheuer, T.; Zheng, N.; Catterall, W. A. *Nature* **2011**, *475*, 353.
20. Schnur, E.; Turkov, M.; Kahn, R.; Gordon, D.; Gurevitz, M.; Anglister, J. *Biochemistry* **2008**, *47*, 911.
21. Otvos, L., Jr; Szendrei, G. I.; Lee, V. M.; Mantsch, H. H. *Eur. J. Biochem.* **1993**, *211*, 249.
22. Wang, K. R.; Zhang, B. Z.; Zhang, W.; Yan, J. X.; Li, J.; Wang, R. *Peptides* **2008**, *29*, 963.
23. Fornili, S. L.; Pizzi, R.; Rebeccani, D. *Int. J. Pept. Res. Ther.* **2010**, *16*, 223.
24. Schwieters, C.; Kuszewski, J.; Tjandra, N.; Clore, G. *J. Magn. Res.* **2003**, *160*, 65.
25. Schwieters, C.; Kuszewski, J.; Clore, G. *Prog. Nucl. Magn. Reson. Spectrosc.* **2006**, *48*, 47.
26. Humphrey, W. *J. Mol. Graphics Modell.* **1996**, *14*, 33.
27. Woody, R.; Tinoco, I. *J. Chem. Phys.* **1967**, *46*, 4927.
28. Wuthrich, K. *Biopolymers* **1983**, *22*, 131.
29. Sarker, M.; Waring, A. J.; Walther, F. J.; Keough, K. M. W.; Booth, V. *Biochemistry* **2007**, *46*, 11047.
30. Linford, N. J.; Cantrell, A. R.; Qu, Y.; Scheuer, T.; Catterall, W. A. *Proc. Natl. Acad. Sci. U.S.A.* **1998**, *95*, 13947.
31. Wang, S. Y.; Wang, G. K. *Biophys. J.* **1999**, *76*, 3141.
32. Codding, P. W. *J. Am. Chem. Soc.* **1983**, *105*, 3172.